# Combined plasma spray and *in situ* laser melting treatment of NiCrBSi powder

N. SERRES[*], F. HLAWKA, S. COSTIL[a], C. LANGLADE[a], F. MACHI[b], A. CORNET

*LGECO – LISS, INSA de Strasbourg, 24 Boulevard de la Victoire, 67000 Strasbourg, France*
*[a]LERMPS – UTBM, site de Sévenans, 90010 Belfort cedex, France*
*[b]IREPA LASER - Pôle API - Parc d'Innovation - 67400 Illkirch, France*

Recently, mechanical industry has been affected by many environmental regulations. For example, hexavalent chromium was prohibited due to its toxicity. Thus it is essential to find new coatings which are able to replace hard chromium plating. In this paper a technique, based on the association between APS (Atmospheric Plasma Spray) and laser melting using a 3kW diode laser is described. This process allows the production of denser coatings with finer structures than as-sprayed coatings. Depending on the processing parameters the mechanical properties, studied by nanoindentation, microhardness measurement and tribological ball-on disc experiments, were improved in terms of hardness and wear resistance.

## 1. Introduction

In order to protect the environment, mechanical engineering as all other industries has to comply with new environmental regulations. Particularly, hexavalent chromium was recently prohibited in the European automotive industry by the end-of-life vehicles directive of the European Parliament. This regulation which applies to the surface treatment industry, reclassified the chromic anhydride among very toxic substances.

Surface coatings by thermal spraying were already developed in industry and some authors obtained good results to replace hard chromium plating [1, 2]. However, mechanical applications are not always satisfactory for reasons of porosity and microstructure. Furthermore, the materials used are often expensive, especially WC-Co. The applications of laser cladding were also studied and allowed the synthesis of denser coatings [3]. But this process presents also a slow velocity of treatment and its efficiency was often criticized. Nowadays, diode lasers, such as the laser used in this study, arouse a great interest. Also, the two processes appear very complementary. In this paper, a technology which combines Atmospheric Plasma Spraying (APS) and laser re-melting in an *in situ* process is described. In order to modify the structure without generating too high level of stress incompatible with mechanical resistance properties, *in situ* coating re-melting appeared as an interesting alternative. In addition, this technology could be another alternative to hard chromium plating, if its mechanical properties are high. A first study was carried out on ceramics coatings [4], and the treatment changed structure from lamellar to dendritic without modifying the elastic response of the deposit. Additionally to decrease the cost of materials, NiCrBSi coatings are broadly used to improve the quality of

components whose surface is subjected to wear and/or corrosion [5], *i.e.* hard chromium plating well-known properties.

Thermal spraying, such as APS presents the advantage of carrying out coatings very quickly (velocity ranging from 60 to 80 m/min depending on the application). Thus it seems interesting to preserve the treatment velocity, if at the same time the microstructure of the coating will be improved by using a laser. The greatest difficulty is to find an agreement between the very high APS process velocity and the laser, in order that the laser can redesign the surface. Indeed, the coating elaboration by laser cladding is carried out at a very low velocity. For example, to cover a steel surface with NiCrBSi powder using laser cladding process, velocity was equal to $1.5 \times 10^{-1}$ m/min according to González *et al.* [6].

The aim of this paper is to find appropriate parameters to develop this *in situ* process for industrial application. Furthermore, a mechanical investigation is carried out by nanoindentation and microhardness measurements to evaluate the improvement of effective Young's elastic modulus and hardness of selected samples. Then, tribological ball-on-disc experiments are also carried out to calculate the wear rate of selected samples and compare them with as-sprayed NiCrBSi coatings.

## 2. Experimental procedure

### 2.1. Feedstock materials

A self-fluxing alloy of high chromium and boron content was investigated in this study. NiCrBSi powder from Höganäs, referenced as grade 1160-00 was used as feedstock material. The sprayed powder composition,

morphology and size distribution are listed in Table I. The powder was sprayed on a C38 steel pin with a diameter of 25 mm and a height of 10 mm. This kind of substrate was used in the experiments. Indeed, the coatings are carried out on the flat surface of the pin (S = 491 mm²).

*Table 1. Chemical composition (wt. %) of spray powder.*

| Chemical composition (wt. %) | | | | | | | Particles size distribution | Morphology |
|---|---|---|---|---|---|---|---|---|
| C | Ni | Fe | Cr | Si | B | O | | |
| 0.76 | 72.33 | 3.87 | 15.16 | 4.65 | 3.19 | 0.043 | ranging from 20 to 63 μm (average 45 μm) | Spherical |

## 2.2. Processing parameters

The experimental device of the hybrid plasma spray process was constituted by the association of a F4 plasma spray gun from Sulzer-Metco and a diode laser (3kW, average power) of 848 nm wavelength, from Laserline (Figure 1). Before the spraying operations, samples were degreased with acetone and alcohol and grit blasted with $Al_2O_3$ to obtain a surface with a mean roughness of about 5 μm. This operation improves the mechanical bonding between the coating and the substrate. Then samples are placed on a holder which has a linear movement and they are swept by the plasma gun and remelted *in situ* by the laser. The coating feedstock material is injected vertically into the plasma jet by Ar carrier gas. The process is carried out at a very high velocity for a laser treatment (v = 75 m/min). Thus, in order to obtain a suitable laser contribution of the process, the area exposed to combined treatment must be small in order to increase the power density at a maximum. Consequently, the laser contribution will be significant. A fixed-focus lens of $0.8 \times 2$ mm² is used, which correspond to the laser beam dimensions. In order to increase the temperature of the sample, the air cooling system is placed at the rear of the holding device. This positioning allows for conservation of the thermal effect provided by the APS. Each sample is treated on all surface area, *i.e.* 491 mm². In this paper three representatives samples are studied. It is assumed that the laser power density and the number of steps have a significant influence on the coating properties. The holding device is fixed on a robot: it moves laterally according to the relative motion and from top to bottom according to the spray step. Therefore, some variations are evaluated, regarding the evolution of the properties of different samples according to the selected processing parameters. The identification of the samples and the processing parameters are given in Tables 2 and 3.
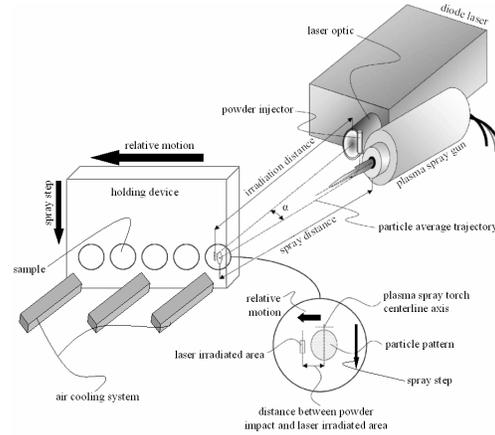


*Fig. 1. Experimental device constituted by the association of a plasma spray gun and a diode laser.*

*Table 2. Selected processing parameters.*

| Parameter | Value |
|---|---|
| Nozzle diameter (mm) | 6 |
| Arc current intensity (A) | 580 |
| Argon flow rate (L/min) | 50 |
| Hydrogen flow rate (L/min) | 8 |
| Feedstock injector diameter (mm) | 1.8 |
| Feedstock injector tip location from gun centerline axis (mm) | 6 |
| Feedstock carrier gas flow rate (Ar) [*] | 1.4 – 1.8 |
| Powder feed rate (g/min) | 25 |
| Spray step (mm) | 3 – 6 |
| Area exposed to plasma spray (mm²) | 30 |
| Area exposed to combined treatment (mm²) | 1.6 |
| Spray distance (mm) | 120 |
| Irradiation distance (mm) | 70 |
| Distance between powder impact and laser irradiation (mm) | 22 |
| α (°) | 13 |
| Spray velocity (m/min) | 75 |

[*] Dependant on the spray step

*Table 3. Nomenclature of selected samples.*

| Sample | Laser power density (W/mm²) | Number of steps (-) |
|--------|------------------------------|---------------------|
| APS | 0 | 8 |
| H1 | 1875 | 4 |
| H2 | 1875 | 8 |
| H3 | 1250 | 8 |

## 2.3. Coatings characterization

### 2.3.1. Microstructure observation

The samples were cut parallel to the spray direction using a diamond saw in an oil medium and mounted in bakelite. Then the cross-sections were polished following standard metallographic techniques *i.e.*, prepolishing and diamond slurry polishing to achieve a final coating roughness of Ra ~ 0.2 µm. Then, the samples were observed using SEM, coupled with energy dispersive spectroscopy (EDS).

The mean roughness, *Ra* (µm) data of samples was calculated by an extended field confocal microscope (STIL's Micromesure station) with a vertical resolution of 0.01 µm and lateral resolution of 2 µm. The topography was measured on a large surface, with a sampling step of 2 µm in the horizontal plan.

Moreover, an assessment of the coating density was made by accurately weighing the samples before and after spraying and then calculating from the volume of the coating deposited. This procedure was undertaken on twelve samples to yield an average value of the layer density.

### 2.3.2. Berkovich nanoindentation

Effective Young's elastic modulus of selected samples was determined using an ultra-low load indentation system equipped with a Berkovich indenter tip (Nano Indenter® XP, MTS Systems Corporation). This microprobe records continuously both the load and the displacement as indents are made on a sample, with resolutions up to 75mN and 0.04 nm, respectively. Thirty indentations were made on selected samples at different loads in the range of 7.5-30mN on coated polished cross-sections. The effective Young's modulus was then calculated from the Oliver-Pharr model [7] and the results were averaged. The Poisson's ratio of different samples was assumed equal to 0.32.

It is also possible to determine the hardness of the coatings with this system, but the samples are thick enough to make standard microhardness measurements. Thus, Vickers hardness measurements were performed on a section perpendicular to the spraying direction with a 100 gf load. These tests provide more reliable information on the influence of laser treatment on the coating hardness.

### 2.3.3. Wear tests

To compare the wear performance of different samples, tribological tests were done. A pin-on-disc type tribometer from CSM Instruments was used for the wear experiments with a sliding distance of 10 km, a sliding speed of 50 cm/s, a ball of 100Cr6 (Ø = 6 mm), under dry-sliding conditions, at atmospheric pressure and room temperature. The normal load, $F_N$, applied on the sample was 2 N. These tests are done on the flat surface of the pin. Four measurements per sample were carried out to ensure the reproducibility of the tests. Before the experiments, the sample surfaces were polished following standard metallographic techniques, *i.e.* prepolishing and diamond slurry polishing. Indeed it is essential to work with a smooth surface in order to decrease the friction efforts between the sample and the counterbody surfaces.

Wear rate was characterized by observing wear scars by microtopography and using SEM. The microtopographic data of wear tracks were obtained by an extended field confocal microscope with a vertical resolution of 0.01 µm and lateral resolution of 2 µm. The topography was measured on a large surface, with a sampling step of 2 µm in the horizontal plan. Finally, the wear coefficient (*K*) was calculated by means of the equation (1) proposed by Archard [8], where *V* is the total wear volume loss (mm$^3$), *P* the applied normal load (N) and *S* the total accumulated displacement (m).

$$K = \frac{V}{P \times S} \qquad (1)$$

## 3. Results and discussion

### 3.1. Coating structure characterization

The coating general microstructures are shown in Fig. 2. Differences in morphology are observed. APS coatings have a lamellar structure and exhibit cracks, pores and unmelted particles, which are emblematic defects for this kind of treatment. The average porosity is about $3.4 \pm 0.3$ % for plasma sprayed coatings [9]. On the contrary, as-sprayed remelted coatings are denser with a dendritic structure and the absence of porosity and microcracks shows that the selected processing parameters have ensured good quality coatings. The thickness of both coatings is comparable, *i.e.* 330 µm for as-sprayed samples and 460 µm for remelted samples. However the surface roughness was changed by the laser treatment. Indeed, there is a reduction of the mean roughness due to laser re-melting: $Ra_{without\ laser}$ = 5.24 µm and $Ra_{with\ laser}$ = 2.91 µm.

a



b
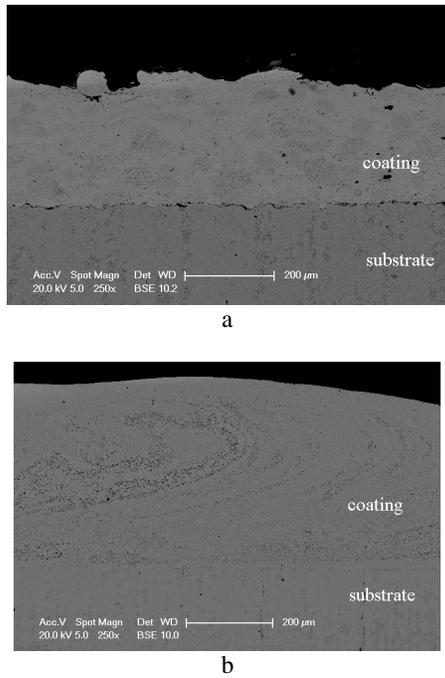
*Fig. 2. General view of NiCrBSi coatings produced by APS (a) and laser melting treatment (b).*

As we can see in Fig. 3, the main result is that the re-melting of the coating reduces porosity and creates a metallurgical bond between the coating and the substrate, which also enhances the cohesion between the particles of the coating, without propagation of cracks. This result is observed for all selected processing parameters. As a consequence, the adhesion will probably strongly increase in comparison with the APS process. Note that the black points in Figure 3b are not porosity but chromium precipitates in a Ni/Si/Fe matrix, such as presented in Figure 4. Furthermore, all remelted samples present finer

structure and higher density than APS coating (Fig. 5). Indeed, as-sprayed sample has a density of 6.64 g/cm$^3$ in comparison with remelted sample which has a density of 8.23 g/cm$^3$. Thus, whatever the irradiance, the microstructure resulting from laser treatment is a dendritic structure.



a



b
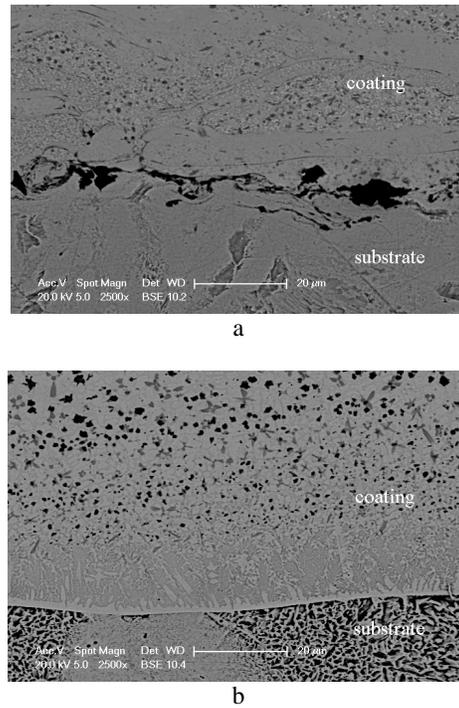
*Fig. 3. Typical interface morphologies of (a) as-sprayed and (b) in situ remelted coating.*
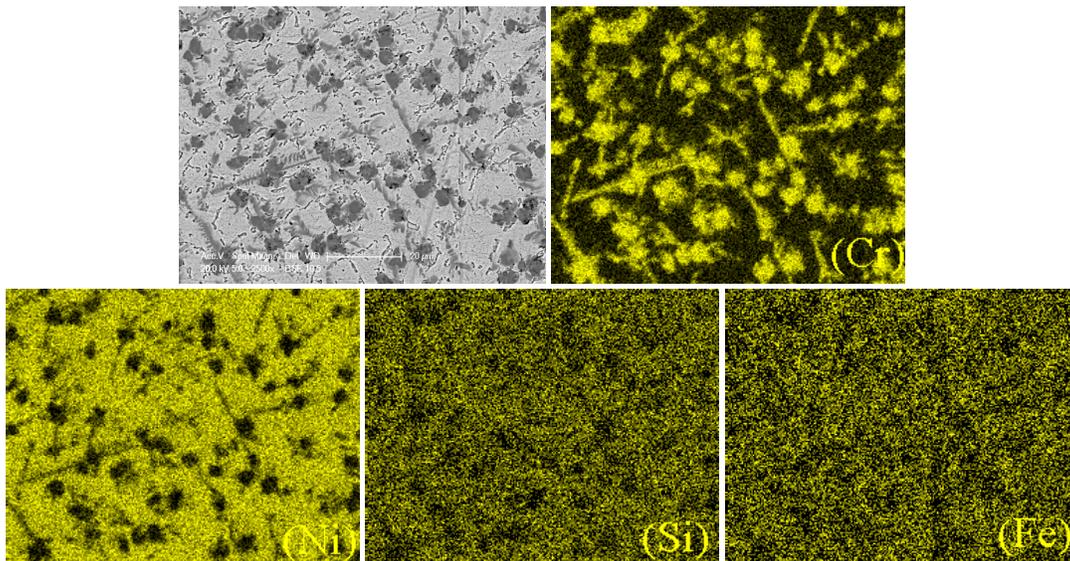


*Fig. 4. Composition of the coating sprayed with Plasma-laser hybrid process carried out by EDS.*

a



b
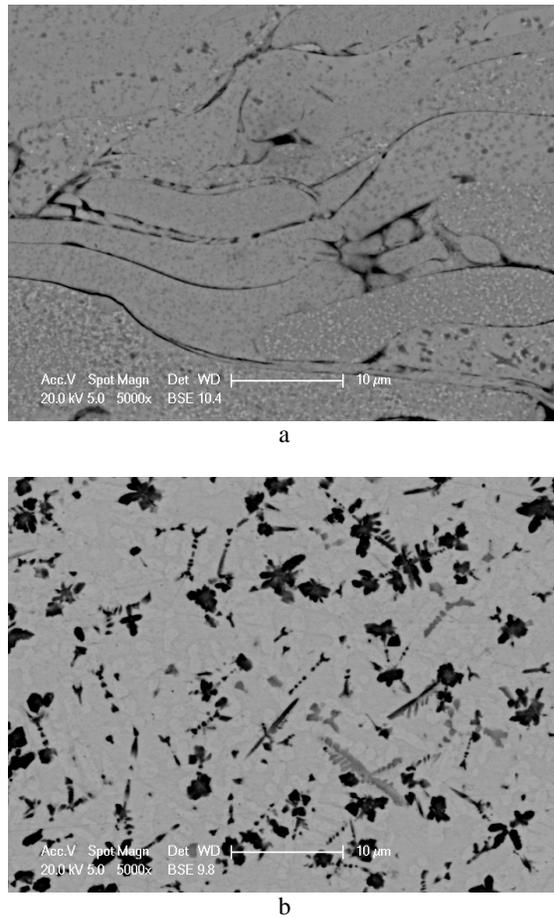
*Fig. 5. Representative cross-section morphologies of (a) as-sprayed and (b) in situ remelted NiCrBSi coatings.*

## 3.2. Mechanical properties

Vickers hardness measurements clearly indicate that the remelted coatings have a higher hardness than the APS coating because of their finer structure and higher density (Fig. 6). Remelted areas with a dendritic structure seem to exhibit a slightly enhanced toughness compared to the lamellar structure of the as-sprayed coating. Indeed, plasma sprayed coatings exhibit lower hardness because of the effect of porosity. The specific comparison between remelted samples demonstrates that the hardness values are increased at the same time as the laser power density and the number of steps.

Load – displacement curves performed with a 30mN load for non-treated and laser treated NiCrBSi allow for comparison of their elastic properties (Figure 6). A little increase in Young's modulus can be verified after *in situ* laser treatment. So, in a first approximation, remelted samples present the same elastic properties as non-treated samples, especially because all samples have a similar chemical composition (Table IV). Indeed, the main difference deals with the presence of oxygen for APS sample due to oxidation during spraying in plasma. The

dimensions of the indented area are several hundred times lower than the average layer cross-section (*i.e.*, ~1μm² versus 750μm², approximately). Thus, the Young modulus determination derived from these measurements is related to the intrinsic or effective modulus, depending on the NiCrBSi structure exclusively and not on the coating architectures. There is also the effect of porosity in case of APS sample, which decreases the cohesion of the coating, improving its elasticity. As a conclusion, the Young's modulus of laser treated samples is higher, with few differences according to the selecting processing parameters.
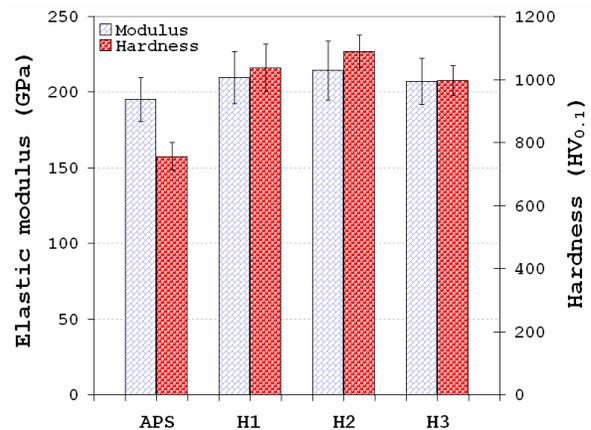


*Fig. 6. Elastic modulus determined using an ultra-low load (30 mN) indentation system equipped with a Berkovich indenter tip and microhardness values of coatings.*

*Table 4. Chemical composition of the coatings obtained by EDS.*

| Wt. (%) | as-sprayed | laser treated |
|---|---|---|
| O | 3.37 | - |
| Si | 4.92 | 5.25 |
| Cr | 11.77 | 13.71 |
| Fe | 5.19 | 7.56 |
| Ni | 74.76 | 73.47 |

## 3.3. Wear experiments

Tribological ball-on-disc experiments are carried out on the APS and remelted samples. Figure 7 shows the wear profiles after ball-on-disk testing for all of the samples. The wear track of the APS coating contains smooth cavities and it seems that some un-melted particles are torn off the coating during the wear test [10]. According to [11], fatigue is the main wear mechanism for this kind of coating and this process is called splat delamination, which is common in thermal sprayed coatings with poor cohesion energy. The porosity of the

APS coating, equal to $3.4 \pm 0.3$ % [9], as well as the cohesion between splats may induce this wear mechanism.
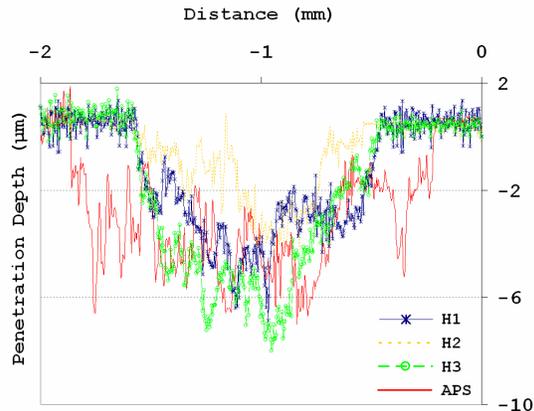


*Fig. 7. Wear profiles after ball-on-disk testing.*
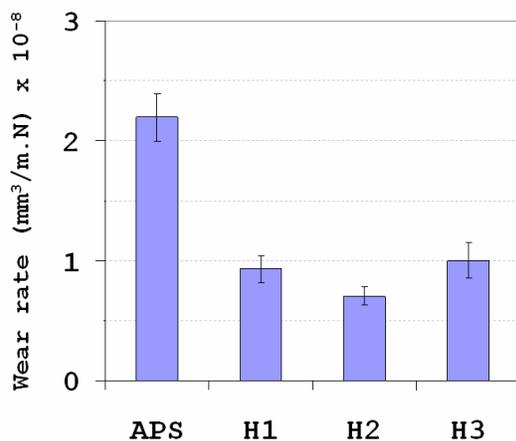


*Fig. 8. Wear rates after ball-on-disk testing.*

Moreover, the wear track profiles of the remelted samples (Fig.7) reveal that the scars are less deep compared to the APS scar. This result is due to improved mechanical properties of remelted coatings as discussed in the previous section. The wear rate of the samples was next calculated using Archard's model (Fig. 8). All values of wear rate are advantageous in case of potential tribological industrial application of these coatings. However the remelted sample types present a better behavior, because of high hardness levels that improve the wear resistance of coatings [11]. Moreover, corresponding to the selected processing parameters the wear rates of the remelted samples are modified. Also, better results are obtained with the sample labeled H2. Thus, the increase of the laser power density coupled with a high number of steps seems to give better results, like with the hardness values observed in Fig. 6.

## 4. Conclusions

The *in situ* process (laser re-melting after plasma spraying) allows the synthesis of denser coatings than APS

with finer structures and without cracks and porosity. The coating is metallurgically bonded to the substrate, which probably will increase the adhesion. Moreover, mechanical properties, especially the hardness are increased and better tribological behavior of the remelted samples can be observed, especially concerning the wear rate of selected samples. Finally, there are some variations according to the selected processing parameters and better mechanical results are obtained with a higher laser power density and elevated number of steps. So this process could be a good alternative to electrolytic hard chrome process due to its good mechanical properties and a specific comparison between these two processes will be carried out soon.

### References

[1] T. Sahraoui, N.E. Fenineche, G. Montavon, C. Coddet, J. Mater. Process. Technol. **152**, 43 (2004).
[2] J. A. Picas, A. Forn, G. Matthäus, Wear **261**, 477 (2006).
[3] L. Pawlowski, J. Therm. Spray Tech. **8**, 279 (1999).
[4] G. Antou, Améliorations de revêtements barrières thermiques par un procédé de refusion laser in situ utilisant un laser à diodes, PhD thesis ULP - INSA de Strasbourg, 2004 (*in french*) (http://eprints-scd-ulp.u-strasbg.fr:8080/123/01/html/index-frames.html)
[5] M. P. Planche, H. Liao, B. Normand, C. Coddet, Surf. Coat. Tech. **200**, 2465 (2005).
[6] R. González, M.A. García, I. Peñuelas, M. Cadenas, M. del Rocío Fernández, A. Hernández Battez, D. Felgueroso, Wear **263**, 619 (2007).
[7] W. C. Oliver, G. M. Pharr, J. Mater. Res. **7**, 1564 (1992).
[8] J. F. Archard, J. Appl. Phy. **24**, 981 (1953).
[9] ASTM International, Test Methods for Determining Area Percentage Porosity in Thermal Sprayed Coatings (2002).
[10] N. Serres, F. Hlawka, S. Costil, C. Langlade, F. Machi, A. Cornet, Surf. Coat. Tech. **204**, 197 (2009).
[11] J. M. Miguel, J. M. Guilemany, S. Vizcaino, Tribo. Int. **36**, 181 (2003).

_____
*Corresponding author : nicolas.serres@insa-strasbourg.fr